

Published in final edited form as:

*Neurobiol Aging*. 2012 June ; 33(6): 1096–1109. doi:10.1016/j.neurobiolaging.2010.09.009.

## Age-related cerebral atrophy in non-human primates predicts cognitive impairments

Jean-Luc Picq<sup>a,b</sup>, Fabienne Aujard<sup>b</sup>, Andreas Volk<sup>c,d</sup>, and Marc Dhenain<sup>e,f,g</sup>

<sup>a</sup> Laboratoire de psychopathologie et de neuropsychologie, E.A. 2027, Université Paris 8, 2 rue de la liberté, 93000 St Denis, France

<sup>b</sup> CNRS UMR 7179, MNHN, 4 Av du Petit Château, 91800 Brunoy, France

<sup>c</sup> Institut Curie, Research Center, 91405 Orsay Cedex, France

<sup>d</sup> U759 INSERM, Centre Universitaire, Labo 112, 91405 Orsay Cedex, France

<sup>e</sup> CEA, DSV, I2BM, MIRCen, URA CEA CNRS 2210, 18 route du panorama 92 265 Fontenay-aux-Roses cedex, France

<sup>f</sup> CNRS, URA 2210, 18 route du panorama 92 265 Fontenay-aux-Roses cedex, France

<sup>g</sup> CEA, DSV, I2BM, NeuroSpin, Centre CEA de Saclay, Bât. 145, 91191 Gif sur Yvette, France

### Abstract

In humans, but not in nonhuman primates, a clear relationship has been established between age-associated cognitive decline and atrophy of specific brain regions. We evaluated age-related cerebral atrophy and cognitive alterations in mouse lemur primates. Cerebral atrophy was evaluated by *in vivo* magnetic resonance imaging in 34 animals aged from 1.9 to 11.8 years. The caudate and splenium were atrophied in most older animals whereas shrinkage of the hippocampus, entorhinal cortex, and septal region was identified in a subgroup of the older animals. The temporal and cingulate cortex also exhibited a severe atrophy whereas frontal and parietal areas were spared. Measures of cognitive ability in 16 animals studied by MRI showed that both executive functions and spatial memory declined with aging. Impairment of executive functions in older animals was associated with atrophy of the septal region while spatial memory performance was related to atrophy of the hippocampus and entorhinal cortex. Mouse lemurs are the first nonhuman primates in which a clear relationship is established between age-associated cognitive alteration and cerebral atrophy.

### Keywords

Aging; Atrophy; Brain; Cognitive disorganization; Imaging

---

Corresponding Author: Marc Dhenain – MIRCen, URA CEA CNRS 2210, 18 route du panorama 92 265 Fontenay-aux-Roses cedex, France. Tel: +33 1 46 54 81 92; Fax: +33 1 46 54 84 51; Marc.Dhenain@cea.fr.

#### Disclosure Statement

Authors have no financial, personal or other conflict of interest to disclose.

Animal studies were performed in accordance with national and international guidelines. In particular, the treatment of animals was in accordance with ethical standards of the statutory order 87 848 (October 13, 1987) of the French Ministry of Agriculture (authorization n° 91-166).

**Publisher's Disclaimer:** This is a PDF file of an unedited manuscript that has been accepted for publication. As a service to our customers we are providing this early version of the manuscript. The manuscript will undergo copyediting, typesetting, and review of the resulting proof before it is published in its final citable form. Please note that during the production process errors may be discovered which could affect the content, and all legal disclaimers that apply to the journal pertain.

## 1. Introduction

In humans, cerebral aging is associated with cognitive impairments and a clear relationship has been established between age-associated cognitive decline and atrophy of specific brain regions (Petersen et al., 2000, Raz et al., 1998, Van Der Werf et al., 2001, Whitwell et al., 2007). For example, during normal aging, perseverative behaviors are correlated to atrophy of frontal regions (Raz et al., 1998). During pathological aging, such as in Alzheimer's disease, memory impairments are strongly associated with atrophy of limbic structures such as the hippocampus (Petersen et al., 2000) or atrophy of the central cholinergic system (Teipel et al., 2005).

Non-human primates can develop age-related cerebral atrophy (Andersen et al., 1999, Dhenain et al., 2003, Dhenain et al., 2000, Kraska et al., In Press). However, unlike in humans, links between regional cerebral atrophy and cognitive alterations have never been reported. The very few studies that have combined behavioral and *in vivo* neuro-anatomical assessments in the same cohort of primates (mainly Macaques) have either failed to find any correlation (Wisico et al., 2008) or found only correlation between cognitive decline and a global cerebral atrophy (Shamy et al., 2006) or between regional atrophy and a performance for a task on which aged monkeys were not impaired (Alexander et al., 2008).

Mouse lemurs are another category of primates. These small nocturnal primates (60-100 g, 12 cm) have a life span of about one decade in captivity. As in all primate species, aged animals display cognitive impairments, especially memory and executive function declines (Gilissen et al., 2000, Picq, 1993, Picq, 1995, Picq and Dhenain, 1998, Picq, 2007). Previous studies, based on measurements of cerebrospinal fluid in ventricles and peri-encephalic areas, have shown cerebral atrophy in lemurs (Dhenain et al., 2003, Dhenain et al., 2000, Kraska et al., In Press). The aim of this study was to evaluate both regional brain volumes and cognitive performances in this primate. *In vivo* magnetic resonance imaging (MRI) detected age-associated regional brain atrophy in a large population of mouse lemurs. Shift tasks and spatial memory tests revealed cognitive alterations in old animals. We showed, for the first time, in non-human primates, correlations between atrophy of specific cerebral structures, especially medio-temporal and septal regions, and cognitive impairments.

## 2. Material and Methods

### 2.1. Subjects

Thirty-four male mouse lemurs (*Microcebus murinus*), born and raised in a laboratory breeding colony in Brunoy, France, underwent MR imaging. The young adult group consisted of 11 animals ranging in age from 1.9 to 2.8 years (mean  $\pm$  SD,  $2.4 \pm 0.4$  y), and the older adult group consisted of 23 animals aged 6.2 to 11.8 years (mean  $\pm$  SD,  $8.0 \pm 1.4$  y). Six of the older animals were involved in earlier MRI studies that took place 1 to 4 years prior to the current work, and their brain images were used for longitudinal analysis. Before entering the study, all animals were checked for health and given an ophthalmologic examination. None of the animals has been previously involved in pharmacological trials.

Sixteen mouse lemurs, five from the young adult group (ages 2.0 to 2.8 y; mean  $\pm$  SD =  $2.6 \pm 0.3$  y) and eleven from the older group (ages 6.2 to 8.4 y; mean  $\pm$  SD,  $7.5 \pm 0.6$ ) also performed cognitive tasks within a maximum period of 4 months before the MRI examination. All animals involved in behavioral evaluation could see well. Given that the mouse lemur exhibits photoperiodically driven seasonal rhythms, they were tested during the long photoperiod (day lengths longer than 12 h), when both behavioral and physiological functions are stimulated. Ambient temperature (24–26°C), relative humidity (55%), and ad libitum food availability were kept constant according to the general conditions of captivity

in the colony. No food deprivation procedure was used during our behavioral tests because the reward consisted in allowing the mouse lemurs to reach their nestboxes. All mouse lemurs were maintained in social groups before and after testing. Because these animals are nocturnal, all tests were performed in a dark room with only dim red light sufficient to see visual stimuli.

## 2.2. MR image acquisition and preprocessing

Brain images were recorded according to previously published protocols (Dhenain et al., 2003) on a 4.7-Tesla Bruker Biospec 47/30 system by using a surface coil (diameter = 30 mm) actively decoupled from the transmitting birdcage probe (Bruker GmbH). Briefly, animals were pre-anesthetized with atropine (0.025 mg/kg subcutaneously) and anesthetized by isoflurane. Respiration rate was monitored to ensure animal stability until the end of the experiment. Body temperature was maintained with a water-filled heating blanket. Three-dimensional inversion-recovery fast spin-echo images were recorded with an isotropic nominal resolution of 234  $\mu\text{m}$  (TR/TE = 2500/6 msec, TE<sub>w</sub> = 45 msec, TI = 200 msec, RARE factor = 16). MR images were zero-filled to reach an apparent isotropic resolution of 117  $\mu\text{m}$ .

Morphometric analyses of the brains were performed using AMIRA software (Mercury Computer Systems Inc., TGS Unit, Villebon, France). Before morphometric analysis, the brain images from the different mouse lemurs were rotated to be positioned in a similar orientation. Standard neuroanatomic landmarks were used to correct deviations in all three orthogonal planes (AMIRA image warping tool): the sagittal plane cut through the middle of the interhemispheric fissure, and the horizontal plane was parallel to the superior border of the median part of the corpus callosum and rigorously perpendicular to the sagittal plane, in accordance with the stereotaxic brain atlas of the grey mouse lemur by Bons et al. (Bons et al., 1998), which was used as a reference for all anatomical landmarks.

## 2.3. Evaluation of brain structure volumes and cortical thickness

Morphometric analyses were performed by measuring the volumes of four brain structures (caudate nucleus, splenium of the corpus callosum, septal region (cholinergic region), and the hippocampus). We chose these structures based on two criteria. First, they are consistently described as deteriorated during aging in the human brain. Second, they were easy to outline because of their clear limits, leading to high measurement reliability. Each structure was manually outlined on coronal sections thanks to a digitizing tablet (AMIRA drawing tools). The detailed procedure and carefully evaluated criteria to outline these structures is provided in supplemental information (Supplementary methods and Supplementary Fig. 1 for the caudate nucleus, Supplementary Fig. 2A for the splenium of the corpus callosum, Supplementary Fig. 2B for the septal region, and Supplementary Fig. 3 for the hippocampus). The quality of the delineation of each structure was checked by examination of axial sections. For each animal the intracranial volume was also evaluated. It was outlined from the most rostral part of the frontal pole to the most caudal part of the occipital pole. This corresponded to an average of 155 coronal sections. The reported volumes for each brain structure (caudate nucleus, splenium, septum, and hippocampus) was normalized by the intracranial volume: For each animal, the reported values for each brain structure corresponded to the volume of the structure divided by the intracranial volume for the mouse lemur, multiplied by the average intracranial volume from all of the mouse lemurs.

The cortical thickness of 12 different cortical areas (grouped as the frontal, parietal, temporal, occipital, and cingulate cortices) was also evaluated (Table 1 and Supplementary Fig. 4).

The measures of brain volumes and cortical thickness were performed by a single experimenter. Intrarater reliability was assessed by measuring each region of interest (ROI) on 10 animals (three from the young group and seven from the older group) on two separate days at least one month apart and by calculation of intraclass correlation coefficients. All the obtained coefficients ranged from 0.99 to 1. The mean measuring error was inferior to 1% for all ROIs and the maximal measuring error inferior to 2%. A second investigator has measured a sample of 6 animals (two from the young group and four from the older group) in order to assess interrater reliability. All interrater reliability values were > 0.90 except the hippocampus ( $\kappa = 0.88$ ).

For longitudinal comparisons, atrophy of a brain structure was defined as a change in volume greater than twice the maximal measuring error for that structure. Any change less than that value was considered non-significant.

## 2.4. Behavioral evaluation by discrimination and shift tasks

**2.4.1. Apparatus description**—All tests were performed in an apparatus especially designed for the mouse lemurs (Fig. 1), consisting of a starting box, a work chamber, and two corridors that could lead to a reinforcement chamber. At the start of each trial, mouse lemurs were put into the starting box and the sliding door of the starting box was removed, allowing the mouse lemur to enter the trapezoidal work chamber illuminated by a red 15-W bulb. The walls of the work chamber were made of plywood, and the ceiling was a one-way mirror that permitted observation of the animal. The base of the larger wall of the work chamber (referred to as the panel choice) comprised two circular openings (diameter, 35 mm) of corridors (length, 25 cm) leading to the reinforcement chamber housing the mouse lemur's usual nest box and sometimes (once in three trials) a piece of fig in a cup. Each corridor could be closed at each end by sliding doors and could be illuminated by a 15-W bulb situated 4 cm above a Plexiglas® window in the ceiling. If the animal entered the positive corridor, the exit door of this corridor was raised, giving access to the reinforcement chamber where the mouse lemur could stay for 2 min. It is worth outlining that during our tests, the main reward consisted in allowing the animals to stay for some time in its nestbox. This reward is particularly efficient in mouse lemurs as they are very keen to find their nestboxes. Notably, the animals were not food deprived. If the animal entered the negative corridor, it was confined in the corridor because the exit door remained shut, and the entrance door was lowered behind it. The mouse lemur was then immediately returned to the starting box for another trial. Four successive tasks were performed in this apparatus: a visual discrimination task (VD), a task of reversion of the visual discrimination (R1), a task of shift of the discriminating stimulus (from visual to spatial: EDS), and a task of reversion of the spatial discrimination (R2). Prior to these tasks, the animals were trained in the apparatus during “habituation sessions.”

**2.4.2. Habituation**—Habituation was performed one day before the evaluated tests. The mouse lemurs were placed in the apparatus for eight trials. In each trial, one single corridor was opened and always gave access to the reinforcement chamber. Over the session, the two corridors were alternatively used. For the first four trials (numbered 1 to 4), the exit door of the corridor was always raised, so that the mouse lemur could quickly go through the corridor to obtain a reward. For the last four trials (5 to 8), the exit door of the corridor was raised once the lemur entered the corridor, so that the mouse lemur had to wait for some time before obtaining access to the reinforcement chamber. For trials 3–4 and 7–8, the corridor was illuminated; for trials 1–2 and 4–5, it was dark.

**2.4.3. Simultaneous Visual Discrimination (VD)**—For all tests (VD, R1, EDS, R2), each day of testing consisted of a maximum of 30 trials comprising presentation of a pair of

corridors. Testing continued until the mouse lemurs reached a criterion of nine correct choices for 10 consecutive trials. For each test, the score was the number of errors before reaching this criterion. Mouse lemurs started a new task the day following success (criterion reached) in a given task.

During the VD, the animals had to discriminate the two corridors based on their illumination. In each trial, only one corridor was illuminated. The location of the illuminated corridor alternated pseudo-randomly, and the choice of the illuminated corridor led to the reward. Thus, only the light held predictive value, and the spatial location of the corridor was irrelevant.

**2.4.4. Task of reversion of the visual discrimination (R1)**—During this shifting task, the reward contingencies were reversed, i.e., the dark corridor was associated with reward.

**2.4.5. Task of shift of the discriminating stimulus (from visual to spatial: extra-dimensional shift (EDS))**—This discrimination comprised the same pair of corridors with the same pseudo-randomized alternation of the illuminated corridors in tasks 1 (VD) and 2 (R1). However, the positive stimulus was now the right corridor, regardless of luminosity. The only novelty was thus that the previously irrelevant dimension became positively or negatively correlated with a reward, requiring a shift of attentional set from visual characteristics (luminosity) to spatial location.

**2.4.6. Task of reversion of the spatial discrimination (R2)**—In this last shifting problem, a response to the corridor on the left was now correct. Thus, the reward contingencies were reversed so that the corridor that was not correlated with a reward (the left corridor) was now positively correlated with a reward and vice versa.

## 2.5. Behavioral evaluation by circular platform test (CPT)

**2.5.1. Apparatus description**—The CPT apparatus was an adaptation for mouse lemurs of the device described by Barnes (1979) (Barnes, 1979). It consisted of a white circular platform (diameter, 100 cm) with 12 equally spaced circular holes (each 5 cm in diameter) located 3 cm from the perimeter (Fig. 1). The platform could be rotated. The maze platform was affixed 60 cm above the floor, and a cardboard nestbox (10 cm × 10 cm × 20 cm) could be inserted and removed beneath each hole and served as a refuge (goal box). A black, small plywood box could be slid beneath the non-goal holes to stop the lemurs from jumping through these holes while permitting head entering. To prevent the mouse lemur from escaping, the platform was entirely surrounded with a white wall 15 cm high across its circumference and covered with a transparent Plexiglas® ceiling that permitted the mouse lemurs to see the extra-maze visual cues. The apparatus was surrounded by a black curtain hung from a square metallic frame (length of the side, 120 cm) located 110 cm above the floor. The center of the frame was a one-way mirror to allow observation. Affixed beneath the one-way mirror and following the circular perimeter of the maze (about 50 cm above the platform) were 24 2-W lights evenly spaced, illuminating the maze. Between the one-way mirror and the upper edge of the wall, various objects were attached along the inner surface of the curtain to serve as visual cues. The starting box was an open-ended dark cylinder positioned in the center of the platform.

**2.5.2. Testing procedure**—During the testing procedure, animals were given one day of habituation and training (day 1) and one day of testing (day 2). Each day comprised four trials, each of which began with placement of the animal inside the starting box at the center of the maze. After 30 s, the box was lifted to release the animal. The aims of the tests were

to reach the goal box positioned beneath one of the 12 holes, kept constant in the room for all trials. When the animal entered the goal box, the trial was stopped, and the animal was allowed to remain in the goal box for 5 min. The platform was randomly rotated on its central axis after each trial to avoid the use of intra-maze cues, although the position of the goal box in the room was kept constant.

On day 1, trials 1 and 2 consisted of placing the animal in a four-walled chamber containing only the opened goal hole (one-choice test). For trials 3 and 4, the platform comprised six evenly spaced open holes (six-choices test). These two trials permitted the animal to explore the maze, observe the visual cues, and further learn the position of the goal box.

On day 2 (testing day), 12 holes were opened during the four trials. Performance was assessed by the number of errors prior to reaching the goal box. An error was defined as an inspection made by inserting the nose into an incorrect hole.

## 2.6. Statistical analyses

Anatomical and behavioral data were analyzed with Mann-Whitney and Spearman's rank correlation coefficients using Statistica v7.1 (StatSoft, Inc., Tulsa, OK, USA). Intraclass correlation coefficients were also calculated by using Statistica v7.1. Profiles of cerebral atrophy were further described by calculating z scores for each brain region. Z scores provide volume/cortical thickness estimates relative to that which would be expected from young (control) animals. Accordingly, for each region evaluated, the profile of z score means for young animals is nearly flat, and the profile of the aged animal reflects regional variation in the extent of volume/cortical thickness abnormalities.

## 3. Results

### 3.1. Reduction of brain structure volumes in aged animals

**3.1.1. Caudate nucleus**—Atrophy of the caudate associated with a dilation of the lateral ventricle that constitutes the medial border of the head of the caudate nucleus was obvious in some animals (Fig. 2A–B). Quantification of the caudate volume showed that it was highly significantly smaller in the older animals as compared to the young adult group ( $U = 18$ ,  $p < 0.001$ ; Fig. 2C). A strong negative correlation also emerged between caudate volume and age ( $r = -0.70$ ,  $p < 0.001$ ). Seemingly, most older lemurs underwent a substantial decline in caudate volume. Indeed, 65% of the young lemurs displayed caudate volume above the range of the older group values, and 63% of values for the older lemur group for caudate volume fell below the range of values for the young group. Thus, the entire range of the older group values was shifted downward relative to the range for the young group. The longitudinal results showed a loss of caudate volume in five out of six mouse lemurs (Fig. 2D).

**3.1.2. Splenium**—Many old mouse lemurs also displayed an obvious atrophy of the splenium. Indeed, in old lemurs this structure did not appear as a caudal enlargement of the corpus callosum as was the case for young animals (Fig. 2E–H). Quantitative study confirmed a significant reduction of the splenium volume in the older group compared to the young animals ( $U = 23$ ,  $p < 0.001$ ; Fig. 2I). There was also a strong negative correlation between age and splenium volume ( $r = -0.66$ ,  $p < 0.001$ ). As with the caudate, atrophy of the splenium seemed widespread among the older animals. Indeed, 57% of the values of splenium volume for the young group were above the range of those for the older group, and 55% of splenium volume values for the older group fell below the range for the young group. Hence, the entire range of values for the older group underwent a downward shift

relative to the range of the young group. The longitudinal measures showed splenium atrophy for five out of the six evaluated mouse lemurs (see Fig. 2J).

**3.1.3. Hippocampus**—Visual inspection also revealed an hippocampal atrophy in some older animals, accompanied by an increase of CSF volume around the hippocampus (Fig. 3A,B). Measurement of hippocampus volumes confirmed a significant decrease of hippocampal volume in older animals compared to young adults ( $U = 54$ ,  $p < 0.01$ ). There was also a significant correlation between hippocampal volume and age ( $r = -0.40$ ,  $p < 0.05$ ; see Fig. 3C). However, the two age groups exhibited a large overlap; indeed, only one young lemur had a hippocampus volume above the range of the older group's values, and only 30% of the older lemurs displayed a hippocampus volume falling below the entire range of values for the young animals. This outcome suggests that only a limited subpopulation of older lemurs underwent hippocampal atrophy. Examination of longitudinal data (Fig. 3D) showed the occurrence of an atrophic process in four out of the six studied animals.

**3.1.4. Septal region**—Finally, the volumes of the septal region in the older animals were smaller than those in young animals ( $U = 49.5$ ,  $p < 0.01$ ; Fig. 3E,F). However, no correlation emerged between septal region volume and age ( $r = -0.31$ ,  $p = 0.07$ , ns). The large overlap between individual measures in young and older animals could explain this result (Fig. 3G). Indeed, only 18% of the young lemurs displayed a septum volume above the range for the older lemurs, and only 34% of the older lemurs had septum volumes falling below the entire range of the young lemur group. As with the hippocampus, these results suggest that only a limited subgroup of older lemurs underwent septal atrophy. Longitudinal data showed an age-related septal region volume loss in five out of the six studied mouse lemurs (Fig. 3H).

### 3.2. Thinner cortex in aged animals

In addition to brain structure volumes, the thickness of 12 cortical regions localized at the level of frontal, parietal, temporal, occipital, and cingulate cortices was measured (Table 1). The older mouse lemurs showed smaller thickness of the anterior (area 24,  $U = 18$ ,  $p < 0.001$ ) and posterior (area 23,  $U = 10$ ,  $p < 0.001$ ) cingulate areas; entorhinal area (area 28,  $U = 52$ ,  $p < 0.01$ ); temporal secondary visual area (area 21,  $U = 27$ ,  $p < 0.001$ ); secondary auditory area (area 22,  $U = 46$ ,  $p < 0.01$ ); occipital secondary visual area (area 18,  $U = 13$ ,  $p < 0.001$ ); and primary visual areas (area 17,  $U = 31$ ,  $p < 0.001$ ) (Fig. 4). The magnitude of the cortical shrinkage in the older group varied greatly among the individual animals and among the different cortical areas but reached to 30% for temporal cortical area 21. By grouping cortical areas into five regions (Table 1), we found that temporal ( $U = 22$ ,  $p < 0.001$ ), cingulate ( $U = 10$ ,  $p < 0.001$ ), and occipital ( $U = 1$ ,  $p < 0.001$ ) cortices were atrophied in older animals compared to young ones while the frontal and parietal cortices were not modified by age. We found a strong correlation between cortical thickness and age for some cortical areas, in particular for the anterior cingulate cortex ( $r = -0.572$ ,  $p < 0.001$ ) (Supplementary Figure 5).

Comparison between hemispheres revealed that the right and left cortices had similar thicknesses in the young adult group but were asymmetric in the older group (Fig. 5, Supplementary Fig. 6). Indeed, among the older lemurs, five left cortical areas were significantly thinner than the same areas in the right cortex: area 4 (rightward asymmetry, right vs. left = 4.8%,  $U = 135$ ,  $p < 0.05$ ), area 18 (right vs. left = 3.6%,  $U = 172$ ,  $p < 0.05$ ), parietal area 5 (right vs. left = 6.8%,  $U = 168$ ,  $p < 0.001$ ), parietal area 7 (right vs. left = 7.2%,  $U = 104$ ,  $p < 0.001$ ), and the entorhinal area 28 (right vs. left = 7.6%,  $U = 161$ ,  $p < 0.05$ ). The thickness of the left cortical areas 5 and 7 was significantly smaller in older animals compared to young animals (for the two areas:  $U = 61$ ,  $p < 0.05$ ).

### 3.3. Profiles of regional volumes and cortical thicknesses

Z scores were used to compare the severity of age-associated atrophy in the various brain regions (Fig. 6). Interestingly, the data revealed the most severe atrophy in the white matter (in the splenium) and in the occipital cortex. Then the most atrophied regions were the caudate nucleus, the septum, the temporal and cingulate cortical regions and to a lesser extent the hippocampus. The frontal and parietal cortical were less atrophied than all the other evaluated regions.

### 3.4. Alterations of behavioral performances in aged animals

**3.4.1. Discrimination and shift tasks: Age associated alterations of executive functions**—Executive functions were evaluated in four successive discrimination tasks: a visual discrimination task based on light discrimination (VD), a task of reversion of the visual discrimination (R1), a task of shift of the discriminating stimulus (from visual to spatial i.e. an extra-dimensional shift EDS), and a task of reversion of the spatial discrimination (R2). Figure 7A shows the number of errors before reaching a criterion of nine correct choices for 10 consecutive trials for each of the four discrimination tasks. No significant difference could be detected between the older and young adult groups on the VD task ( $U = 23.5$ ,  $p > 0.05$ ). Age was not correlated to performance on this task, either ( $r = 0.018$ ,  $p > 0.05$ ). On the R1 task, older mouse lemurs were significantly impaired ( $U = 1$ ,  $p < 0.01$ ). Likewise, on the EDS task, older animals made more errors than the young adults ( $U = 6.5$ ,  $p < 0.05$ ), and on the R2 task, the older animals performed below the entire range of scores for the young group ( $U = 0$ ,  $p < 0.01$ ). By grouping the scores of the EDS task with those of the two reversal tasks, we calculated a shifting set ability score (SSAS) and found a severe age-related deficit ( $U = 0$ ,  $p < 0.01$ ). A correlation emerged between behavioral performance and age for shift tasks (evaluated by the SSAS) ( $r = 0.60$ ,  $p < 0.05$ ).

**3.4.2. Circular platform test**—Spatial memory was evaluated in the circular platform test (CPT). As shown in Figure 7B, the mean percentage of errors was 1.8 for the young adult group and 6.3 for the older group. The difference was significant ( $U = 10$ ,  $p < 0.05$ ), but a large individual variability emerged within the older group, with some of the older animals performing as well as younger ones, whereas other older animals were severely impaired. We identified a correlation between age and performance ( $r = 0.67$ ,  $p < 0.01$ ).

### 3.5. Cognitive performance are correlated to regional brain volumes in aged animals

In the older group, performance on shift tests, evaluated by the SSAS, was correlated with the septal region volume ( $r = 0.61$ ,  $p < 0.05$ , Fig. 8A). In addition, the performance on the CPT was significantly and positively correlated to hippocampus volume ( $r = 0.60$ ,  $p < 0.05$ , Fig. 8B) and entorhinal cortex thickness ( $r = 0.61$ ,  $p < 0.05$ , Fig. 8C). To assess the specificity of these relationships, we checked that there were no other significant correlations with other brain regions.

In the young adult group, no correlation emerged between cognitive scores and brain volumes.

Among all animals, scores to the shift task, evaluated by the SSAS, were correlated to the volume of the septal region ( $r = 0.75$ ,  $p < 0.001$ ); the caudate ( $r = 0.55$ ,  $p < 0.05$ ) and the splenium ( $r = 0.69$ ,  $p < 0.01$ ) and to the thickness of the anterior ( $r = 0.71$ ,  $p < 0.01$ ) and posterior ( $r = 0.54$ ,  $p < 0.05$ ) cingulate cortices; the associative visual cortical areas 21 ( $r = 0.76$ ,  $p < 0.001$ ) and 18 ( $r = 0.66$ ,  $p < 0.01$ ). Scores to the CPT were correlated to volume of the hippocampus ( $r = 0.52$ ,  $p < 0.05$ ) and the thickness of the entorhinal cortex ( $r = 0.76$ ,  $p < 0.001$ ).



## 4. Discussion

### 4.1. Age associated cerebral atrophy

MRI evaluations in lemurs revealed an age-related cerebral atrophy in white matter regions, in the caudate nucleus, in cholinergic, and in cortical and hippocampal regions. White matter region such as the splenium was the most strongly atrophied in older animals compared to young ones. Caudate nucleus was also particularly atrophied in old animals. In addition, there was a significant correlation between the volume of these structures and age. The septal region was also severely atrophied in aged lemurs as compared to young ones although a large overlap was detected between the size of this structure for the two age groups. This suggests that only a limited subpopulation of older lemurs underwent a septal atrophy. The severity of cortical/hippocampal atrophy was more region-dependent. The most atrophied regions were the temporal, cingulate, occipital and hippocampal regions, while the fronto-parietal regions were less impaired. For the temporal cortex including the entorhinal region, and the hippocampus a large overlap was however seen between the sizes of these structures for the two age groups. This suggests that only a limited subpopulation of older lemurs underwent atrophy of medio-temporal structures. The atrophy of the cingulate and occipital cortex in old animals was obvious from our analysis of the profiles of regional volumes. Also, an age-associated cortical thinning was detected in the anterior cingulate cortex.

Our results are consistent with studies showing that atrophy of the caudate is a robust finding associated with normal aging in humans (Gunning-Dixon et al., 1998, Jernigan et al., 1991), as well as in nonhuman primates (Matochik et al., 2000). Concerning the white matter, data from human studies are controversial. It has been described as either undergoing a widespread age-associated decline in volume (Resnick et al., 2003) or as showing no age-related significant atrophy (Good et al., 2001). On the other side, in primates such as rhesus monkeys, an age-related alteration in myelin sheaths of the splenium has been reported (Peters, 2002). Our results thus further suggest that white matter is a brain region that is particularly sensitive to age effects in primates.

Our data also showed atrophy of septal region only in a subgroup of older animals, suggesting that atrophy of cholinergic regions in mouse lemurs is linked to pathological aging. This result is consistent with data in humans showing a marked loss and/or shrinkage of the cholinergic cells of the basal forebrain during pathological aging conditions such as AD (Teipel et al., 2005, Whitehouse et al., 1981). During normal aging in humans data are more controversial as some article found no obvious atrophy of cholinergic regions (Chui et al., 1984) while some other found an alterations of these regions (Lowes-Hummel et al., 1989). Data in other primates such as macaques are also controversial as some studies (Smith et al., 2004), but not all (Voytko et al., 1995) found an age-associated loss of cholinergic neurons in the nucleus basalis of Meynert.

In humans, an atrophy of medio-temporal regions has been described during normal aging (Jack et al., 1998, Petersen et al., 2000) but has not, however, been reported in all studies (Salat et al., 2004). Medio-temporal atrophy is more prominent during pathological aging such as AD (Jack et al., 1998). In contrast with data from humans, no age-related atrophy of hippocampus was found in macaques (Shamy et al., 2006) despite cognitive impairments mimicking those resulting from hippocampal damage are observed only in a subpopulation of aged monkeys (Rapp and Amaral, 1991). The lack of medio-temporal atrophy in macaques can be explained by the very small number of aged subjects used in macaque studies due to practical constraints (Shamy et al., 2006). Our study is thus the first one to show age-related hippocampal and entorhinal atrophy in primates. The occurrence of such

atrophy in a sub-population of aged animals, suggests that as in humans, it might be associated to pathological aging processes.

Finally, our study revealed that the left hemisphere exhibited a greater rate of thinning than the right hemisphere. This type of left-sided pattern of cerebral atrophy has been previously reported in AD (Boxer et al., 2003, Whitwell et al., 2007); thus, this result in lemurs also is reminiscent of pathological aging in humans.

#### 4.2. Relationship between behavioral alterations and regional brain atrophy

The behavior of mouse lemurs was evaluated by using two different tasks: the shift task and the circular platform test.

In the shift tasks, all of the older animals were impaired with no overlap between young and older group scores. The failing of old animals in shift tasks was not the result of an inability to perform visual discriminations but of difficulties in reversing or shifting previous discriminations. Such age-related behavioral rigidity has been widely described in both human and animal studies and is considered as a fundamental sign of cognitive aging (Barense et al., 2002, Dempster, 1992, Moore et al., 2003). Within the older group where most animals were of a similar age (thus removing the confounding factor of age in interpretation), impairment in shift tasks correlated with atrophy of the septal region. Such a correlation is consistent with data showing that degeneration of the ascending cholinergic projections results in cognitive dysfunction (Collerton, 1986, Samuel et al., 1994). Indeed, ascending cholinergic projections control the cortical activation required for efficient processing of afferent information. Also the cholinergic basal forebrain promotes cognitive flexibility; for example, rats with medial septal lesions become unable to use a “non-stereotypic strategy” to solve the radial maze (Janis et al., 1994). In a recent formulation of the functions of the cholinergic system, cholinergic inputs to the cortex have been described as enhancing attention to sensory stimuli and encoding new memories while reducing or suppressing internal processing of previously stored information (Hasselmo and McGaughy, 2004). Our findings of reduced flexibility in shifting tasks in older mouse lemurs with septal region atrophy are thus consistent with these data.

In the circular platform test, the performance of most older mouse lemurs matched that of the younger animals, but some of the older animals were severely impaired. This data is consistent with studies in other animals showing a great behavioral variability in aged animals as compared to young ones (Zola-Morgan, 1993). In our study, none of the young animal was impaired. One can expect that in a larger population, some young animal would not do well on cognitive tests. We probably did not detect such animals because of the low number of young animals tested. Interestingly, performances in the circular platform test in old animals were correlated with atrophy level of the hippocampus or the entorhinal cortex. Our data thus suggest that atrophy of the medio-temporal lobe in a subgroup of older animals has functional consequences. This relationship between medio-temporal lesions and performance on the circular platform test is consistent with results from a host of anatomo-functional studies in rodents (McLay et al., 1999, McNaughton et al., 1989).

It is worth emphasizing that the mouse lemurs are the only nonhuman primates reproducing the link between regional cerebral atrophy and age-associated cognitive alterations. Atrophied regions linked to cognitive alterations in our tests are cholinergic regions, as well as hippocampo-entorhinal regions.

The origin of the neurodegenerative processes associated to cognitive alterations occurring in lemurs still remains to be discovered. Because of the close phylogenetic relationship between lemurs and humans and because we evaluated spontaneously occurring aging in

lemurs, findings in lemurs are expected to be directly transposable to human studies. Recently, we highlighted a link between intracellular amyloid deposition, neuroinflammation and cerebral atrophy (Kraska et al., In Press). Other age-associated cerebral alterations occurring in lemurs should also be investigated to explain cognitive aging in these animals. For example, age-associated iron accumulation (Dhenain et al., 1998), possibly leading to oxidative stress can lead to cognitive alterations reported in aged-lemurs. Other lesions such as amyloid plaques are of particular interest in lemurs (Bons et al., 1991, Mestre-Francés et al., 1996). Indeed, studies based on small animal cohort showed that 5 to 8 percent of the 5 to 9 year-old animals develop a significant number of plaques. This value reaches 40% of the animals older than 10 years (Mestre-Frances et al., 2000). Typically, plaques are detected in the cortical regions with a highest load in the temporal region, an intermediate load in the frontal and parietal cortexes and the lowest load in the occipital cortex (Mestre-Frances et al., 2000). The numerous plaques from the temporal cortex, a region that was atrophied in our old animals, are rather small and compact (Mestre-Frances et al., 2000), and are considered as mature plaques. Plaques from the frontal and parietal cortexes, two regions that were not atrophied in our study, are larger and more diffuse, and thus less mature (Mestre-Frances et al., 2000). In lemurs, age-associated amyloid deposits also occur as amyloid angiopathy. This lesion is confined mostly to leptomeningeal vessel walls close to the surface of the brain and is rarely present in intracortical capillary walls. So far, no regional specificity has been described for this lesion (Mestre-Frances et al., 2000).

Neurofibrillary changes are other lesions of interest described in aged lemurs. They can be dissociated into age-associated changes of intracellular Tau accumulation and changes of pTau accumulation. Data on Tau accumulation suggest an age-specific increase of Tau proteins in the frontal, parietal, occipital and temporal cortexes (Giannakopoulos et al., 1997). Regarding pTau, a recent study described intraneuronal accumulation of pTau, labeled with specific antibodies such as CP13, in the hippocampus, but not in the cortex (Kraska et al., In Press). However, no study based on a large cohort of animals outlined the frequency and location of the pTau pathology. The relationship between atrophy, cognitive alterations and pTau pathology will thus have to be further studied.

Other microscopic alterations that have been associated to cognitive alterations in other non-human primates should also be studied. For example synaptic loss in prefrontal cortex (Peters et al., 2008), microcolumnar organization loss in prefrontal cortex (Cruz et al., 2009), degeneration of myelinated fibers in prefrontal cortex (Peters et al., 1994) or alterations of neurotransmitters (Mestre and Bons, 1993, Smith et al., 2004) should be investigated.

## 5. Conclusion

This study has produced four major findings. First, mouse lemurs exhibit widespread brain shrinkage with age. Second, this shrinkage is not uniform. Its magnitude varies across brain regions and across individuals, as is consistently described in humans. Third, some atrophy processes occur in almost all older animals, specifically in the splenium and caudate nucleus. Some other atrophies (of the hippocampus, entorhinal cortex, and septal region) concern only a subgroup of older animals suggesting their association with a pathologic process. Fourth, the atrophies in the latter regions are correlated with changes in cognitive performance. Interestingly, in humans, these regions are severely altered in pathological aging processes such as AD. All of these results suggest that mouse lemurs mimic more than other tested primates the pattern of cerebral aging described in humans, in particular the relationships between regional cerebral atrophy and cognitive decline and, therefore, confirm the potential of the mouse lemur as a useful animal model for human brain aging.

These findings also show that MRI and behavioral studies provide valid biomarkers for following age-related cerebral alterations in this primate.

## Supplementary Material

Refer to Web version on PubMed Central for supplementary material.

## Acknowledgments

We thank Benoît Delatour for a critical reading of the article. This work was supported by the Aging ATC 2002 (INSERM), the Fédération pour la Recherche sur le Cerveau 2003, the ACI Neurosciences 2004 (French Research Department), the France-Alzheimer association, the longevity program from the CNRS, the National Foundation for Alzheimer's Disease and Related Disorders, and the National Institute on Aging (R01-AG020197).

## References

- Alexander GE, Chen K, Aschenbrenner M, Merkley TL, Santerre-Lemmon LE, Shamy JL, Skaggs WE, Buonocore MH, Rapp PR, Barnes CA. Age-related regional network of magnetic resonance imaging gray matter in the rhesus macaque. *J Neurosci*. 2008; 28(11):2710–2718. [PubMed: 18337400]
- Andersen AH, Zhang ZM, Zhang M, Gash DM, Avison MJ. Age-associated changes in rhesus CNS composition identified by MRI. *Brain Res*. 1999; 829(1-2):90–98. [PubMed: 10350533]
- Barense MD, Fox MT, Baxter MG. Aged rats are impaired on an attentional set-shifting task sensitive to medial frontal cortex damage in young rats. *Learn Mem*. 2002; 9(4):191–201. [PubMed: 12177232]
- Barnes CA. Memory deficits associated with senescence: a neurophysiological and behavioral study in the rat. *J Comp Physiol Psychol*. 1979; 93(1):74–104. [PubMed: 221551]
- Bons N, Mestre N, Petter A. Senile plaques and neurofibrillary changes in the brain of an aged lemurian primate, *Microcebus murinus*. *Neurobiol Aging*. 1991; 13:99–105. [PubMed: 1542387]
- Bons N, Sihol S, Barbier V, Mestre-Frances N, Albe-Fessard D. A stereotaxic atlas of the grey lesser mouse lemur brain (*Microcebus murinus*). *Brain Res Bull*. 1998; 46(1, 2):1–173. [PubMed: 9639030]
- Boxer AL, Rankin KP, Miller BL, Schuff N, Weiner M, Gorno-Tempini ML, Rosen HJ. Cinguloparietal atrophy distinguishes Alzheimer disease from semantic dementia. *Arch Neurol*. 2003; 60(7):949–956. [PubMed: 12873851]
- Chui HC, Bondareff W, Zarow C, Slager U. Stability of neuronal number in the human nucleus basalis of Meynert with age. *Neurobiol Aging*. 1984; 5(2):83–88. [PubMed: 6493436]
- Collerton D. Cholinergic function and intellectual decline in Alzheimer's disease. *Neuroscience*. 1986; 19(1):1–28. [PubMed: 3537837]
- Cruz L, Roe DL, Urbanc B, Inglis A, Stanley HE, Rosene DL. Age-related reduction in microcolumnar structure correlates with cognitive decline in ventral but not dorsal area 46 of the rhesus monkey. *Neuroscience*. 2009; 158(4):1509–1520. [PubMed: 19105976]
- Dempster FN. The rise and fall of the inhibitory mechanism: Toward a unified theory of cognitive development and aging. *Dev Review*. 1992; 12(1):45–75.
- Dhenain M, Chenu E, Hisley CK, Aujard F, Volk A. Regional atrophy in the brain of lissencephalic mouse lemur primates: measurement by automatic histogram-based segmentation of MR images. *Magn Reson Med*. 2003; 50(5):984–992. [PubMed: 14587009]
- Dhenain M, Duyckaerts C, Michot JL, Volk A, Picq JL, Boller F. Cerebral T2-weighted signal decrease during aging in the mouse lemur primate reflects iron accumulation. *Neurobiol Aging*. 1998; 19(1):65–69. [PubMed: 9562505]
- Dhenain M, Michot JL, Privat N, Picq JL, Boller F, Duyckaerts C, Volk A. MRI description of cerebral atrophy in mouse lemur primates. *Neurobiol Aging*. 2000; 21(1):81–88. [PubMed: 10794852]
- Giannakopoulos P, Sihol S, Jallageas V, Mallet J, Bons N, Bouras C, Delaere P. Quantitative analysis of tau protein-immunoreactive accumulations and beta amyloid protein deposits in the cerebral

- cortex of the mouse lemur, *Microcebus murinus*. Acta Neuropathol. 1997; 94:131–139. [PubMed: 9255387]
- Gilissen, EP.; Dhenain, M.; Allman, JM. Brain aging in Strepsirhine Primates. In: Hof, PR.; Mobbs, CV., editors. Functional Neurobiology of Aging. Academic Press; San Diego: 2000. p. 421-433.
- Good CD, Johnsrude IS, Ashburner J, Henson RN, Friston KJ, Frackowiak RS. A voxel-based morphometric study of ageing in 465 normal adult human brains. Neuroimage. 2001; 14(1 Pt 1): 21–36. [PubMed: 11525331]
- Gunning-Dixon FM, Head D, McQuain J, Acker JD, Raz N. Differential aging of the human striatum: a prospective MR imaging study. AJNR Am J Neuroradiol. 1998; 19(8):1501–1507. [PubMed: 9763385]
- Hasselmo ME, McLaughly J. High acetylcholine levels set circuit dynamics for attention and encoding and low acetylcholine levels set dynamics for consolidation. Prog Brain Res. 2004; 145:207–231. [PubMed: 14650918]
- Jack CRJ, Petersen RC, Xu Y, O'Brien PC, Smith GE, Ivnik RJ, Tangalos EG, Kokmen E. Rate of medial temporal lobe atrophy in typical aging and Alzheimer's disease. Neurology. 1998; 51:993–999. [PubMed: 9781519]
- Janis LS, Bishop TW, Dunbar GL. Medial septal lesions in rats produce permanent deficits for strategy selection in a spatial memory task. Behav Neurosci. 1994; 108(5):892–898. [PubMed: 7826512]
- Jernigan TL, Archibald SL, Berhow MT, Sowell ER, Foster DS, Hesselink JR. Cerebral structure on MRI, part I: Localisation of age-related changes. Biol Psychiatry. 1991; 29:55–67. [PubMed: 2001446]
- Kraska A, Dorieux O, Picq JL, Petit F, Bourrin E, Chenu E, Volk A, Perret M, Hantraye P, Mestre-Frances N, Aujard F, Dhenain M. Age associated cerebral atrophy in mouse lemur Primates. Neurobiol Aging. In Press. 10.1016/j.neurobiolaging.2009.05.018
- Lowes-Hummel P, Gertz HJ, Ferszt R, Cervos-Navarro J. The basal nucleus of Meynert revised: the nerve cell number decreases with age. Arch Gerontol Geriat. 1989; 8(1):21–27.
- Matochik JA, Chefer SI, Lane MA, Woolf RI, Morris ED, Ingram DK, Roth GS, London ED. Age-related decline in striatal volume in monkeys as measured by magnetic resonance imaging. Neurobiol Aging. 2000; 21:591–598. [PubMed: 10924777]
- McLay RN, Freeman SM, Harlan RE, Kastin AJ, Zadina JE. Tests used to assess the cognitive abilities of aged rats: their relation to each other and to hippocampal morphology and neurotrophin expression. Gerontology. 1999; 45(3):143–155. [PubMed: 10202259]
- McNaughton BL, Barnes CA, Meltzer J, Sutherland RJ. Hippocampal granule cells are necessary for normal spatial learning but not for spatially-selective pyramidal cell discharge, Experimental brain research. Experimentelle Hirnforschung. 1989; 76(3):485–496. [PubMed: 2792242]
- Mestre-Francés N, Keller E, Calenda A, Barelli H, Checler F, Bons N. Immunohistochemical analysis of cerebral cortical and vascular lesions in the primate *Microcebus murinus* reveal distinct amyloid beta 1-42 and beta 1-40 immunoreactivity profiles. Neurobiology of Disease. 2000; 7(1):1–8. [PubMed: 10671318]
- Mestre-Francés N, Silhol S, Bons N. Evolution of  $\beta$ -amyloid deposits in the cerebral cortex of *Microcebus murinus* lemurian primate. Alzheimer Res. 1996; 2:19–28.
- Mestre N, Bons N. Age-related cytological changes and neuronal loss in basal forebrain cholinergic neurons in *Microcebus murinus* (Lemurian primate). Neurodegeneration. 1993; 2:25–32.
- Moore TL, Killiany RJ, Herndon JG, Rosene DL, Moss MB. Impairment in abstraction and set shifting in aged rhesus monkeys. Neurobiol Aging. 2003; 24(1):125–134. [PubMed: 12493558]
- Peters A. The effects of normal aging on myelin and nerve fibers: a review. J Neurocytol. 2002; 31(8-9):581–593. [PubMed: 14501200]
- Peters A, Leahu D, Moss MB, McNally KJ. The effects of aging on area 46 of the frontal cortex of the rhesus monkey. Cereb Cortex. 1994; 4(6):621–635. [PubMed: 7703688]
- Peters A, Sethares C, Luebke JI. Synapses are lost during aging in the primate prefrontal cortex. Neuroscience. 2008; 152(4):970–981. [PubMed: 18329176]
- Petersen RC, Jack CR, Xu YC, Waring SC, O'Brien PC, Smith GE, Ivnik RJ, Tangalos EG, Boeve BF, Kokmen E. Memory and MRI-based hippocampal volumes in aging and AD. Neurology. 2000; 54(3):581–587. [PubMed: 10680786]

- Picq JL. Radial maze performance in young and aged grey mouse lemurs (*Microcebus murinus*). *Primates*. 1993; 24(2):223–226.
- Picq JL. Effects of aging upon recent memory in *Microcebus murinus*. *Aging Clin Exp Res*. 1995; 7(1):17–22.
- Picq JL, Dhenain M. Reaction to new objects in young and aged grey mouse lemurs (*Microcebus murinus*). *Q J Exp Psychol - B*. 1998; 51(4):337–348.
- Picq JL. Aging affects executive functions and memory in mouse lemur primates. *Exp Gerontol*. 2007; 42(3):223–232. [PubMed: 17084573]
- Rapp PR, Amaral DG. Recognition memory deficits in a subpopulation of aged monkeys resemble the effects of medial temporal lobe damage. *Neurobiol Aging*. 1991; 12(5):481–486. [PubMed: 1770984]
- Raz N, Gunning-Dixon FM, Head D, Dupuis JH, Acker JD. Neuroanatomical correlates of cognitive aging: evidence from structural magnetic resonance imaging. *Neuropsychology*. 1998; 12(1):95–114. [PubMed: 9460738]
- Resnick SM, Pham DL, Kraut MA, Zonderman AB, Davatzikos C. Longitudinal magnetic resonance imaging studies of older adults: a shrinking brain. *J Neurosci*. 2003; 23(8):3295–3301. [PubMed: 12716936]
- Salat DH, Buckner RL, Snyder AZ, Greve DN, Desikan RS, Busa E, Morris JC, Dale AM, Fischl B. Thinning of the cerebral cortex in aging. *Cereb Cortex*. 2004; 14(7):721–730. [PubMed: 15054051]
- Samuel W, Terry RD, DeTeresa R, Butters N, Masliah E. Clinical correlates of cortical and nucleus basalis pathology in Alzheimer dementia. *Arch Neurol*. 1994; 51(8):772–778. [PubMed: 8042925]
- Shamy JL, Buonocore MH, Makaron LM, Amaral DG, Barnes CA, Rapp PR. Hippocampal volume is preserved and fails to predict recognition memory impairment in aged rhesus monkeys (*Macaca mulatta*). *Neurobiol Aging*. 2006; 27(10):1405–1415. [PubMed: 16183171]
- Smith DE, Rapp PR, McKay HM, Roberts JA, Tuszynski MH. Memory impairment in aged primates is associated with focal death of cortical neurons and atrophy of subcortical neurons. *J Neurosci*. 2004; 24(18):4373–4381. [PubMed: 15128851]
- Teipel SJ, Flatz WH, Heinsen H, Bokde AL, Schoenberg SO, Stockel S, Dietrich O, Reiser MF, Moller HJ, Hampel H. Measurement of basal forebrain atrophy in Alzheimer's disease using MRI. *Brain*. 2005; 128(Pt 11):2626–2644. [PubMed: 16014654]
- Van Der Werf YD, Tisserand DJ, Visser PJ, Hofman PA, Vuurman E, Uylings HB, Jolles J. Thalamic volume predicts performance on tests of cognitive speed and decreases in healthy aging. A magnetic resonance imaging-based volumetric analysis. *Brain Res Cogn Brain Res*. 2001; 11(3):377–385. [PubMed: 11339987]
- Voytko ML, Sukhov RR, Walker LC, Breckler SJ, Price DL, Koliatsos VE. Neuronal number and size are preserved in the nucleus basalis of aged rhesus monkeys. *Dementia*. 1995; 6(3):131–141. [PubMed: 7620525]
- Whitehouse PJ, Price DL, Clark AW, Coyle JT, DeLong MR. Alzheimer disease: evidence for selective loss of cholinergic neurons in the nucleus basalis. *Ann Neurol*. 1981; 10(2):122–126. [PubMed: 7283399]
- Whitwell JL, Przybelski SA, Weigand SD, Knopman DS, Boeve BF, Petersen RC, Jack CR Jr. 3D maps from multiple MRI illustrate changing atrophy patterns as subjects progress from mild cognitive impairment to Alzheimer's disease. *Brain*. 2007; 130(Pt 7):1777–1786. [PubMed: 17533169]
- Wisco JJ, Killiany RJ, Guttmann CR, Warfield SK, Moss MB, Rosene DL. An MRI study of age-related white and gray matter volume changes in the rhesus monkey. *Neurobiol Aging*. 2008; 29(10):1563–1575. [PubMed: 17459528]
- Zola-Morgan S. A perspective on behavioral studies in aged monkeys. *Neurobiol Aging*. 1993; 14(6):647–648. [PubMed: 8295673]

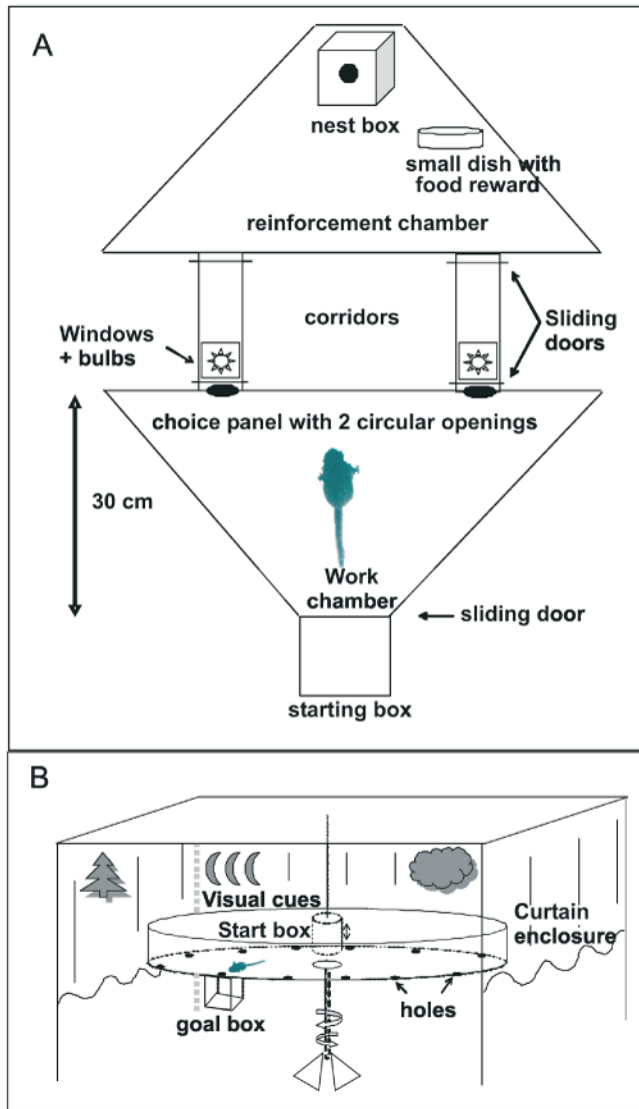


**Figure 1.** Apparatus used in mouse lemurs for discrimination and shifting tasks (A) and for circular platform test (B).

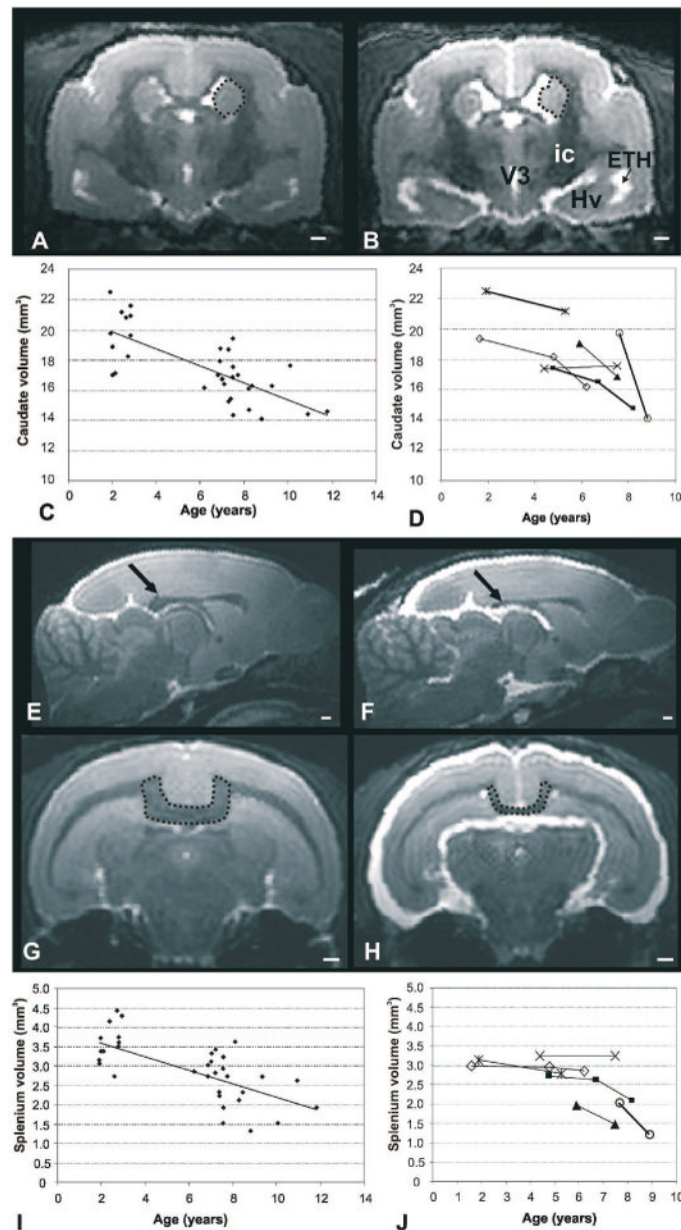


**Figure 2.**

Changes in caudate (A-D) and splenium (E-J) volumes as a function of age.

(A-B) MRI Coronal section showing the shrinkage of the caudate (right caudate outlined by the dotted line) between 5.9 (A) and 7.5 years (B) in a mouse lemur. (C) Cross-sectional data with regression line. (D) Longitudinal follow up of the caudate for six mouse lemurs. (E-H) MRI sagittal (E, F) and coronal (G, H) sections, at the level of the splenium of the corpus callosum (indicated with arrows on sagittal images and outlined with dotted lines on coronal images). E and G, 2.4-year-old mouse lemur; F and H, 8.8-year-old mouse lemur. (I) Cross-sectional data with regression line. (J) Longitudinal follow up of the splenium for six mouse lemurs. Abbreviations: ic = internal capsule, ETH = external part of the temporal horn of the lateral ventricle, Hv = ventral hippocampus, V3 = third ventricle. Scale bars: 1mm.



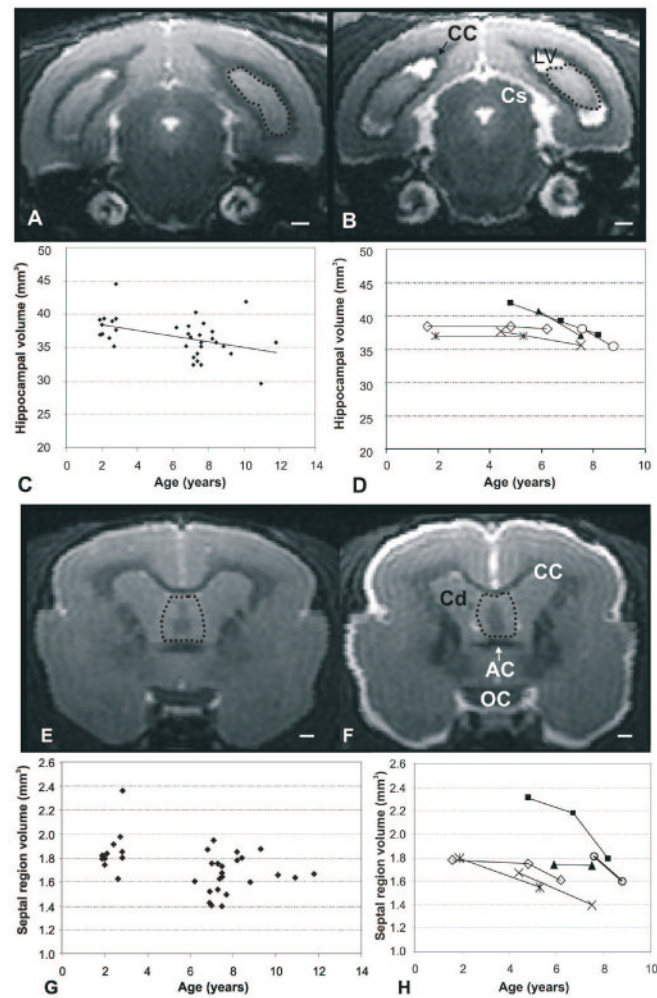


**Figure 3.** Changes in hippocampal and septal region volumes as a function of age. (A-B) MRI coronal sections, at the level of caudal hippocampus (outlined with dotted lines on the right hemisphere), of a 2-year-old (A) and a 7.5-year-old (B) mouse lemur. (C) Cross-sectional data with regression line. (D) Longitudinal follow up of hippocampal volumes for six mouse lemurs. (E-F) MRI coronal sections, at the level of septal region (outlined with dotted lines), of a 2.5-year-old (E) and a 8.5-year-old (F) mouse lemur. (G) Cross-sectional data with regression line. (H) Longitudinal follow up of the septal volumes for six mouse lemurs. Abbreviations: AC = anterior commissure, CC = corpus callosum, Cd = caudate, Cs = colliculus superior, Lv = lateral ventricle, OC = optic chiasm. Scale bars: 1mm.

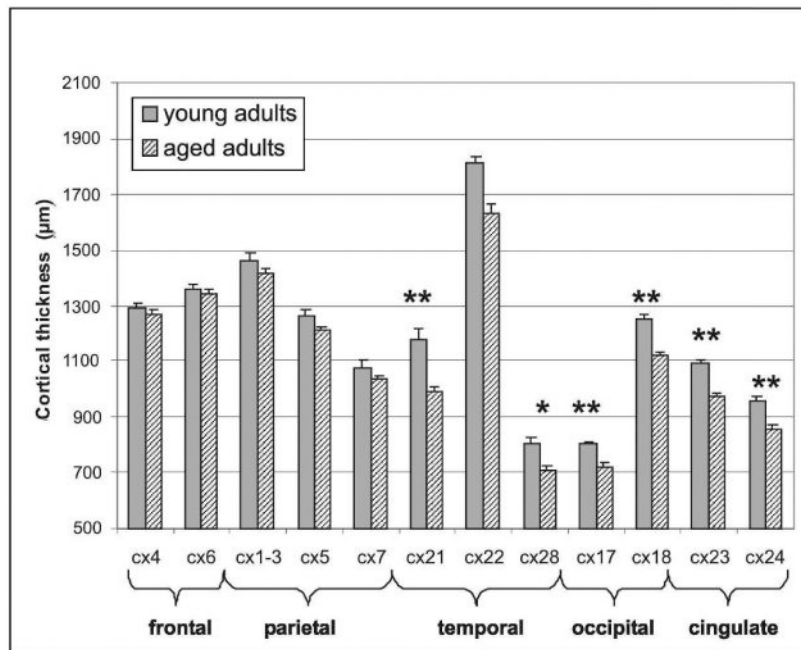


**Figure 4.**

Age-related change in cortical thickness.

Mean cortical thickness (+ S.E.M.) of twelve cortical areas for the young and the aged group. Asterisk indicates a significant difference between the two groups (\* =  $p < 0,01$ ; \*\* =  $p < 0,001$ ). Cx 4: primary motor area. Cx 6: secondary motor area. Cx 1-3: primary somatosensory area. Cx 5: secondary somatosensory area. Cx 7: multimodal sensory area. Cx 21: secondary visual area. Cx 22: secondary auditory area. Cx 28: entorhinal area. Cx 17: primary visual area. Cx 18: secondary visual area. Cx 23: posterior cingulate area. Cx 24: anterior cingulate area.

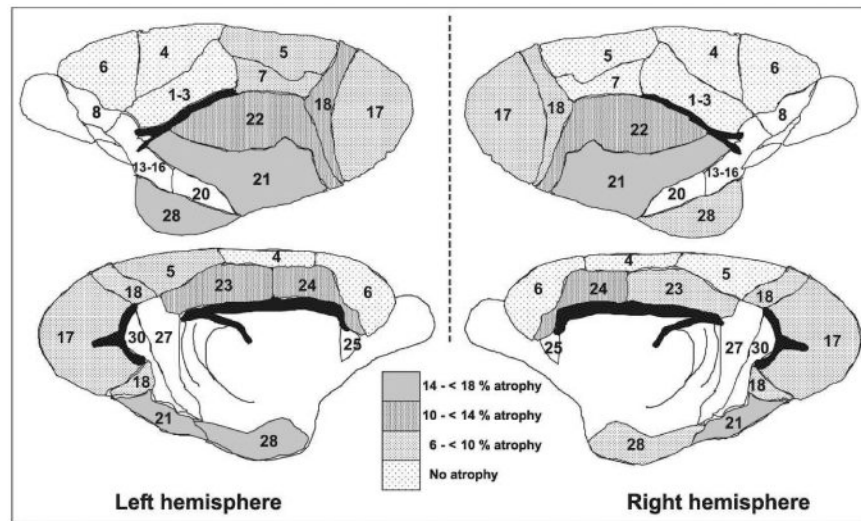


**Figure 5.** Maps of cortical atrophy in the older adult group. Lateral views of each hemisphere are shown at the top and medial views at the bottom. Not measured cortical areas are left in white. Patterns indicate the mean thinning rate for each measured cortical area.

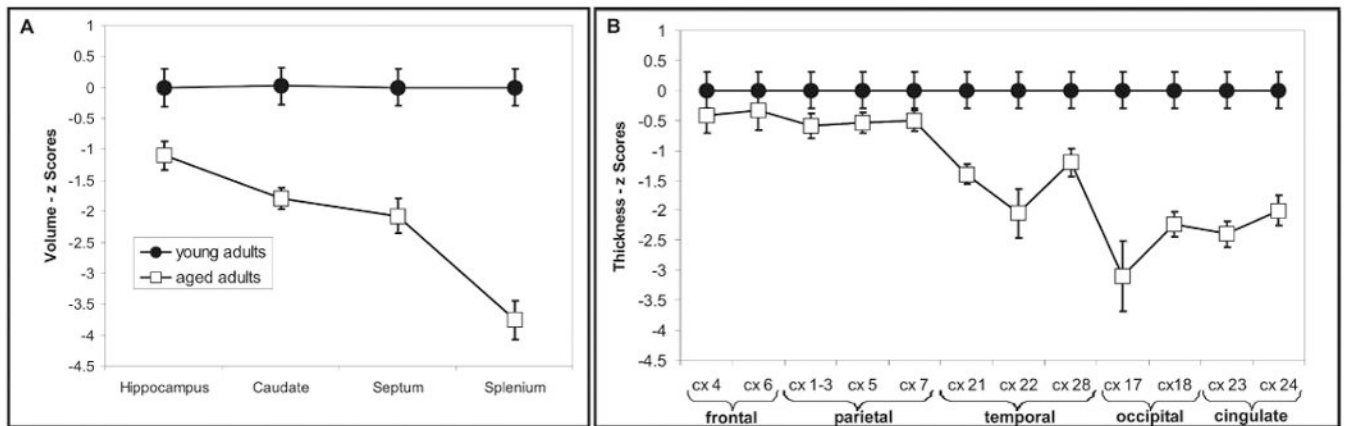


**Figure 6.** Profile of regional volumes (A) and cortical thicknesses (B) expressed as mean  $\pm$  SEM z scores for the two age groups. In aged lemurs, atrophy was particularly severe in the splenium and occipital cortex. The hippocampus, caudate, septum, temporal and cingulate cortex were also particularly atrophied in aged lemurs. Frontal and parietal cortices were less atrophied.

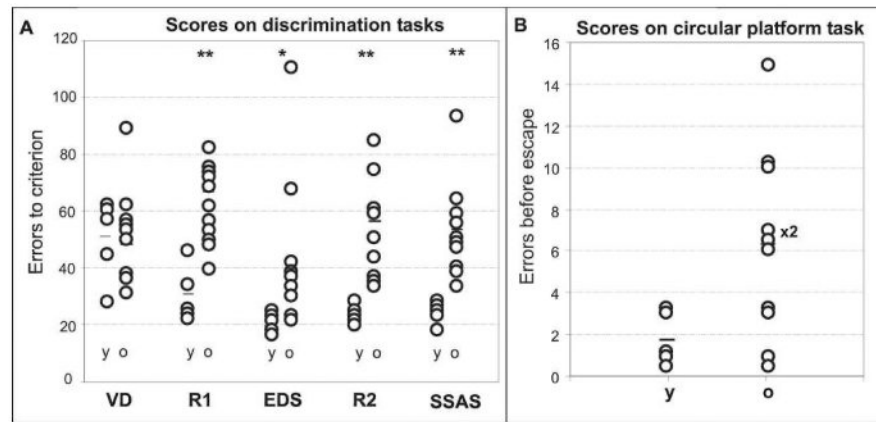


**Figure 7.**

A. Mean errors to criterion on the four discrimination tasks and for the shifting set ability score in young (y) and older (o) animals. VD, Visual Discrimination acquisition; R1, first Reversal discrimination; EDS, Extra-Dimensional Shift; R2, second Reversal discrimination; SSAS, shifting set ability score. Black symbols represent the individual scores. Small horizontal lines show the mean score for each group. Asterisks indicate a significant difference between groups (\*\*:  $p < 0.01$ , \*:  $p < 0.05$ ). B. Performance of young (y) and older (o) adult mouse lemurs in the circular platform task. Black symbols represent the individual scores ( $\times 2$  = number of ties). Small horizontal lines indicate the mean score for each group.

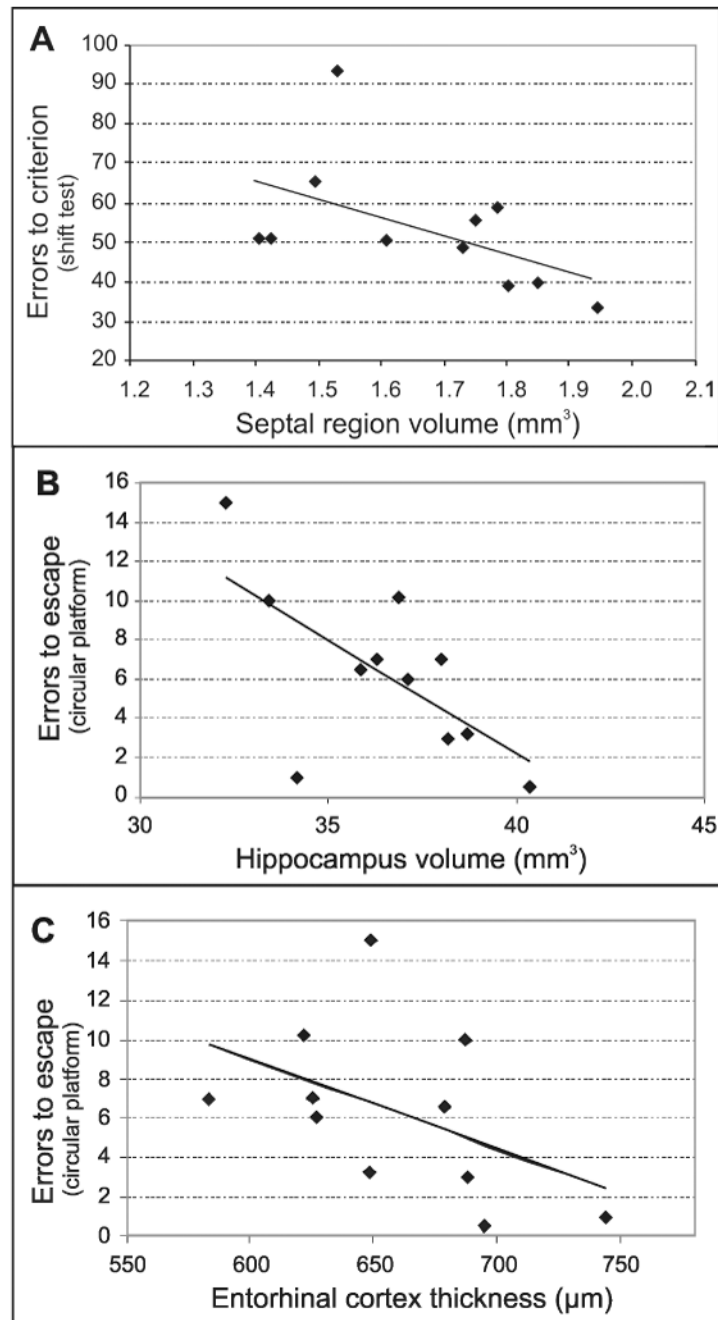


**Figure 8.** Scatterplots and regression lines showing correlations between cognitive performances and brain measures in the older group. (A) Shift tests were correlated with septal region volumes. (B-C) Circular platform task was correlated with hippocampus volume (B) and entorhinal cortex thickness (C).

**Table 1**

List of the cortical areas measured.

Frontal lobe	Area 4	Primary motor area	Temporal lobe	Area 21	Secondary visual area
	Area 6	Secondary motor area		Area 22	Secondary auditory area
Parietal lobe	Area 1-3	Primary somatosensory area	Occipital lobe	Area 28	Entorhinal area
	Area 5	Secondary somatosensory area		Area 17	Primary visual area
	Area 7	Multimodal sensory area		Area 18	Secondary visual area
	Area 23	Posterior cingulate area			
Cingulate lobe	Area 24	Anterior cingulate area			